Linear Stability and the Braess Paradox in Coupled Oscillators Networks and Electric Power Grids

Tommaso Coletta and Philippe Jacquod
School of Engineering, University of Applied Sciences of Western Switzerland, CH-1951 Sion, Switzerland
(Dated: April 6, 2016)

We investigate the influence that adding a new coupling has on the linear stability of the synchronous state in coupled oscillators networks. Using a simple model we show that, depending on its location, the new coupling can lead to enhanced or reduced stability. We extend these results to electric power grids where a new line can lead to four different scenarios corresponding to enhanced or reduced grid stability as well as increased or decreased power flows. Our analysis shows that the Braess paradox may occur in any complex coupled system, where the synchronous state may be weakened and sometimes even destroyed by additional couplings.

PACS numbers: 05.45.Xt, 88.80.hh, 88.80.hm

I. INTRODUCTION.

Collective synchrony is an omnipresent phenomenon in systems of coupled oscillators [1, 2]. It arises when the coupling between individual oscillators becomes strong enough that it overcomes the tendency of oscillators to swing at their natural frequencies. Simplified models such as the Kuramoto model [1, 3] allow to describe a plethora of non linear phenomena involving collective synchrony in Josephson junction arrays [4], biological systems [5, 6], crowd dynamics [7], coupled neural networks [8], chemical reactions [9] and electric power grids [10–13] to name but a few. Quite naturally, one expects that adding couplings between initially uncoupled pairs of oscillators generically favors synchrony. This is however not always the case, Nishikawa and Motter provided analytical conditions for systems of coupled oscillators to be synchronizable over a larger parameter range [14]. References [15, 16] found numerically that adding a new coupling in an initially synchronous system sometimes destroys synchrony. This unexpected scenario is the electrical analog of the Braess paradox, first discussed in the context of traffic networks [17, 18], where building new roads sometimes increases traffic congestions. Similar counterintuitive observations were reported for simple mechanical systems and uncontrolled electric circuits [19, 20]. One purpose of the present manuscript is to present a more systematic analytical treatment of the Braess paradox in coupled oscillator systems. While our focus is on electric power grids, our theory also applies to other oscillator networks described by similar models.

The operational state of AC power grids requires synchrony of thousands of rotating machines of widely varying sizes, millions of electric and electronic devices and components, over several voltage levels intercoupled by frequency-preserving transformers [21]. Nowadays, power grids are maintained in a synchronous state at their rated frequency (50 or 60 Hz) by active control of power generators. An inbalance between production and consumption results in a variation of the operating frequency but not necessarily in the loss of synchrony. The latter may arise if frequency variations exceed safety margins that require to disconnect parts of the network. The standard operational protocol is crucially challenged by the current rise of weakly controllable renewable energy sources. Maintaining the operational state and guaranteeing the safe distribution of power under these changing circumstances requires power grid upgrades, in particular the addition of new transmission lines. This is however both costly and not always well accepted socially. It is therefore crucial to upgrade grids efficiently, adding as few lines as possible to ensure a more stable and safer grid operation. Understanding the Braess paradox in electric power systems is therefore key to optimize the grid of tomorrow.

Improvement in grid operation after a line addition can be quantified for instance by (i) the new power flows on initially strongly loaded lines, this measure of power re-routing is related to line outage distribution factors used in electrical engineering [22], (ii) the linear stability as measured by the Lyapunov spectrum [12, 23–26] of the upgraded grid and (iii) the size of the basin of attraction of the synchronous state in the associated parameter space [27]. Further criteria include N-1 feasibility and voltage stability [21]. In this work we investigate the impact of line addition on grid operation along points (i) and (ii) in a purely reactive power grid. We illustrate analytically on a simple chain network how the perturbative addition of a line, which modifies the grid topology by creating a loop, affects the power load of the electrical connections and the linear stability. We classify the impact of the new line into one of four different scenarios - depending on whether linear stability is improved or not, and whether strongly loaded power lines are relieved or not. Out of these four possible scenarios, three are different manifestations of the electrical Braess paradox, where (I) already strongly loaded lines become even more strongly loaded, (II) network stability is reduced or (III) both. We furthermore show how these three scenarios for the Braess paradox also occur in a complex network having the topology of the British electric transmission grid. Our analytical calculation contributes to the understanding of the Braess paradox in electrical systems. We conjecture that the paradox is generic and may occur in any system of coupled oscillators with reduced connectivity.

II. THE CHAIN MODEL.

We consider an AC electric power system in the form of a chain connecting $N+1$ nodes [see Fig. 1]. A unique generator (labeled $i=0$) is located at one end of the branch while the remaining N nodes (labeled $i=1,\ldots,N$) are all loads. A

necessary condition for the system to be in steady state is that the total injected power at the generator is equal to the total power consumed by the loads. For a power injection $P_0 > 0$ at the generator and $P_i < 0$ at the loads, in arbitrary units, this amounts to $\sum_{i=0}^{N} P_i = 0$. As is the case for high voltage transmission grids, the line admittance is dominated by the susceptance (its imaginary part). Accordingly we neglect ohmic effects and assume that each node has a constant internal voltage magnitude $|V_i|$. Under these approximations the active power flow equations read [15, 21, 28–31]

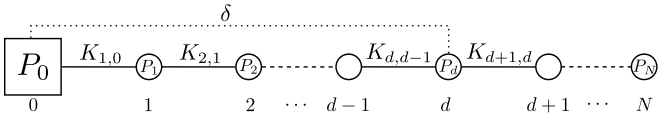

FIG. 1. The chain model. A single generator (square) injects a power $P_0 > 0$ which is consumed by N loads (circles) each consuming a power of $P_i < 0$ in arbitrary units. The lines have capacity $K_{i+1,i} \geq P_0 - \sum_{l=1}^{i} |P_l|$, except the newly added line (dotted) which has capacity δ.

$$0 = P_i + \sum_{j\sim i} K_{i,j} \sin\left(\theta_j - \theta_i\right) \quad i \in \{0, 1, \ldots, N\} \,, \tag{1}$$

where $j \sim i$ indicates that the sum over j spans the nodes connected to the i^{th} node, $K_{i,j} = K_{j,i} = B_{i,j}|V_i||V_j|$ denotes the maximum power capacity of line $\langle i, j\rangle$ having susceptance $B_{i,j}$ and θ_i is the voltage angle (with respect to the current) at node i. Since $P_i^\star = P_0 - \sum_{l=1}^{i} |P_l|$ units of power are transmitted from node i to $i+1$, the line capacities must satisfy $K_{i+1,i} \geq P_i^\star$ for Eqs. (1) to have a solution. Solving Eqs. (1) for the angles yields

$$\theta_{i+1,i} \equiv \theta_{i+1} - \theta_i = -\arcsin\left[P_i^\star / K_{i+1,i}\right] \quad i \in \{0, 1, \ldots, N-1\} \,, \tag{2}$$

so that $\theta_{i+1,i} \in [-\pi/2, 0]$.

We next add to this topology a line of capacity δ between the generator and the d^{th} load, $d \in \{1, \ldots, N\}$. When $\delta \ll K_{i+1,i}$ for all i, the perturbed solution $\{\tilde{\theta}_i\}$ remains close to the unperturbed one, i.e. $\tilde{\theta}_{i+1,i} \approx \theta_{i+1,i} + \epsilon_{i+1,i}$ with $|\epsilon_{i+1,i}| \ll 1$. Solving for the $\epsilon_{i+1,i}$'s, one obtains explicitly the 1^{st} order correction to the unperturbed power flow solution as

$$\epsilon_{i+1,i} = \begin{cases} -\dfrac{\delta}{K_{i+1,i}} \dfrac{\sin\theta_{d,0}}{\cos\theta_{i+1,i}} & 0 \leq i \leq d-1 \,, \\ 0 & i \geq d \,. \end{cases} \tag{3}$$

Clearly, $\epsilon_{i+1,i} = 0$ for $i \geq d$ since the power flowing through the lines connecting nodes i and $i+1$ for $i \geq d$ is left unchanged. Since the above result is valid to 1^{st} order in δ/K, all angle differences entering Eq. (3) are differences of the unperturbed angles $\{\theta_i\}$. In particular, the difference between the voltage angles of the nodes which are connected by the new line is $\theta_{d,0} = \sum_{i=0}^{d-1} (\theta_{i+1} - \theta_i) = -\sum_{i=0}^{d-1} \arcsin\left[P_i^\star / K_{i+1,i}\right]$. Below we investigate how the power flowing through the lines changes when adding the new line.

III. IMPACT OF LINE ADDITION ON POWER FLOWS.

To leading order in δ/K, the power flowing through the additional line is $P_{d,0} = \delta \sin\theta_{d,0}$ [32]. The sign of $P_{d,0}$, and thus the direction of the power flow, changes as a function of d. The power flowing through the $\langle 0, 1\rangle$ line between the generator and the first node goes from $P_{1,0} = K_{0,1}\sin\theta_{1,0} = -P_0$ to $\tilde{P}_{1,0} = K_{1,0}\sin\tilde{\theta}_{1,0} \approx -P_0 - \delta\sin\theta_{d,0}$ once the new line is added. As long as $\sin\theta_{d,0} \leq 0$, the new line lowers the load on all the lines $\langle i, i+1\rangle$ for $i = 0, \ldots, d-1$. However, when $\sin\theta_{d,0} \geq 0$, we face the counterintuitive situation where the new line transmits power back from node d to the generator, thereby increasing the load on all the lines between the generator and node d in the original network. This is an electric manifestation of the Braess paradox [17, 18] and its occurrence is due to the nonlinear nature of the power flow Eqs. (1). In the case of our simple model, which of these two scenarios takes place depends only on the value of $\theta_{d,0}$.

IV. LINEAR STABILITY.

The solutions of the power flow Eqs. (1) describe the operating stationary state of the power grid at a given time. Upon changing conditions, such as variations of the power injected and consumed, the angles' dynamics in this transient stability problem is governed by the *swing equations* [13, 21]

$$I_i\ddot{\theta}_i + D_i\dot{\theta}_i = P_i + \sum_{j\sim i} K_{i,j} \sin\left(\theta_j - \theta_i\right) \,, \tag{4}$$

which describe the power balance at nodes with rotating machines as generators or loads. Without inertia $I_i \equiv 0$, Eqs. (4) reduce to a Kuramoto-like model [1, 3, 33], with reduced connectivity. Linear stability in the Kuramoto and similar models with reduced connectivity has been investigated in Refs. [30, 34–36], which derived bounds on the exponential rate of return to the stationary state.

For $I_i \neq 0$, linearizing Eq. (4) around a stationary solution $\boldsymbol{\Theta}(t) = \boldsymbol{\theta} + \boldsymbol{\delta\theta}(t)$ yields the eigenvalue equation

$$M\boldsymbol{\delta\theta} = \Lambda\left[\Lambda\mathrm{diag}(\mathbf{I}) + \mathrm{diag}(\mathbf{D})\right]\boldsymbol{\delta\theta} \,, \tag{5}$$

where $\Lambda's \in \mathbb{C}$ are the Lyapunov exponents of the dynamics governed by Eq. (4), $\mathrm{diag}(\mathbf{I})$ and $\mathrm{diag}(\mathbf{D})$ are diagonal matrices, $\mathrm{diag}(\mathbf{I})_{ii} = I_i$ and $\mathrm{diag}(\mathbf{D})_{ii} = D_i$. Finally, M is the stability matrix defined by $M_{ij} = K_{i,j}\cos\theta_{j,i}$ if i and j are connected, $M_{ii} = -\sum_{l\sim i} M_{i,l}$ and zero otherwise [12, 23]. The stationary solution is linearly stable if the largest nonzero Lyapunov exponent is negative and unstable otherwise. We next show that the system is stable if M is negative semidefinite and that the loss of stability occurs when the largest nonzero eigenvalue of M becomes positive. This justifies our use of the spectrum of M as measure of stability, keeping in mind that time scales, e.g. for restoring synchrony may depend on I_i and D_i.

In the case of homogeneous inertia $I_i \equiv I$ and damping coefficients $D_i \equiv D$, Eq. (5) is diagonalized by the eigenvectors

of M and the Lyapunov exponents are simply given by

$$\Lambda_a^{\pm} = -\frac{\beta}{2} \pm \frac{1}{2}\sqrt{\beta^2 + 4\lambda_a I^{-1}}\,, \tag{6}$$

where $\beta = D/I$ and λ_a is one of the eigenvalues of the stability matrix M. In the inhomogeneous case, projecting Eq. (5) onto $\boldsymbol{\delta\theta}$ gives,

$$0 = \Lambda^2 a + \Lambda b - c\,, \tag{7}$$

where we introduced the shorthand notation for the overlaps $a = \boldsymbol{\delta\theta}\mathrm{diag}(\mathbf{I})\boldsymbol{\delta\theta}$, $b = \boldsymbol{\delta\theta}\mathrm{diag}(\mathbf{D})\boldsymbol{\delta\theta}$ and $c = \boldsymbol{\delta\theta}M\boldsymbol{\delta\theta}$, with coefficients $a, b \geq 0$ since inertia and damping coefficients are positive quantities (i.e. $D_i, I_i \geq 0\ \forall i$). The Lyapunov exponents then take the form

$$\Lambda^{\pm} = \frac{1}{2a}\left(-b \pm \sqrt{b^2 + 4ac}\right). \tag{8}$$

In both Eqs. (6) and (8), $\mathrm{Re}[\Lambda^-]$ is always negative and stability depends on the sign of $\mathrm{Re}[\Lambda^+]$.

In the homogenous case, Eq. (6) makes it clear that linear stability is determined uniquely by the spectrum of M: $\mathrm{Re}[\Lambda_a^+]$ and λ_a become positive simultaneously. Since M is real and symmetric, all λ_a's are real. Thus, the necessary condition for the system to be stable is that all λ_a are negative. Furthermore, $\mathrm{Re}[\Lambda_a^+]$ is negative and decreasing as λ_a decreases in the interval $0 > \lambda_a > -I\beta^2/4$, while $\mathrm{Re}[\Lambda_a^+]$ saturates at $-\beta/2$ when λ_a is decreased further. Thus, not too far from loss of stability, the spectrum of M is as good a measure of increase/decrease of stability as the true Lyapunov spectrum.

We extend the approach of Ref. [26], which deals with inhomogeneous damping but identical inertia, to the case of inhomogenous inertia and damping. When M is negative semidefinite, the coefficient c in Eq. (8) is negative. Thus, given that $a \geq 0$, $\mathrm{Re}[\Lambda^+]$ is negative and the solution is linearly stable. Furthermore, the cancellation of the Lyapunov exponent occurs only when c vanishes. For this to take place, $\boldsymbol{\delta\theta}$ must be proportional to one of the eigenvectors of M associated to a zero eigenvalue. This shows that a stationary solution of the dynamic system (4) is linearly stable as long as M is negative semidefinite and the loss of stability occurs when the largest nonzero eigenvalue of M vanishes.

We therefore take from now on the spectrum of M as a measure for increased (λ_a decreases) or decreased stability (λ_a increases). Because inertia does not influence the stationary state, taking this latter criterion allows to make more general statements regarding stability, however one needs to keep in mind that I_i and D_i may in principle affect stability in a nontrivial way. We defer investigations of this issue to future work.

Having discussed the role of the spectrum of the stability matrix on the Lyapunov exponents we next investigate how stability is affected as a line is added to an initially stable network.

V. LINEAR STABILITY FOR THE CHAIN MODEL

In the case of the chain model prior to line addition, M is a $(N+1)\times(N+1)$ tridiagonal, symmetric matrix.

$$M = -\begin{pmatrix} C_{1,0} & -C_{1,0} & 0 & \dots & 0 \\ -C_{1,0} & C_{1,0}+C_{2,1} & -C_{2,1} & 0 & \vdots \\ 0 & \ddots & \ddots & \ddots & 0 \\ \vdots & 0 & \ddots & \ddots & -C_{N,N-1} \\ 0 & \dots & 0 & -C_{N,N-1} & C_{N,N-1} \end{pmatrix}, \tag{9}$$

where $C_{j,i} \equiv K_{j,i}\cos\theta_{j,i}$. Since $\theta_{i+1,i} \in [-\pi/2, 0]$, M is diagonally dominant [37] with only negative diagonal elements and positive subdiagonal elements. It thus belongs to the family of Jacobi matrices [38], in particular M has distinct eigenvalues. By Gershgorin circle theorem [39], it is negative semi-definite. Furthermore, $\mathbf{u}^{(1)} = (1, \dots, 1)$ is the eigenvector associated to the eigenvalue which vanishes by rotational invariance. We order the eigenvalues of M as $\lambda_1 = 0 > \lambda_2 > \dots > \lambda_{N+1}$. The semi-negativity of the stability matrix indicates that the power flow solution of the original network topology is stable against small perturbations. Since the largest eigenvalue λ_1 vanishes, stability is determined by λ_2. Next, we therefore calculate the leading order correction to λ_2 resulting from the line addition.

The stability matrix $\tilde{M}$ after the new line has been added, has a very similar structure to M except that, first, the angles entering in $\tilde{M}$ are the $\tilde{\theta}_i$'s and second, the new line modifies the following matrix elements: $\tilde{M}_{1,1} = -\tilde{C}_{1,0} - \tilde{C}_{d,0}$, $\tilde{M}_{d+1,1} = \tilde{M}_{1,d+1} = \tilde{C}_{d,0}$ and $\tilde{M}_{d+1,d+1} = -\tilde{C}_{d-1,d} - \tilde{C}_{d+1,d} - \tilde{C}_{d,0}$, where $\tilde{C}_{j,i} \equiv K_{ij}\cos\tilde{\theta}_{j,i}$ and $K_{d,0} = K_{0,d} = \delta$. Using Eq. (3), we express $\tilde{M}$ as $\tilde{M} = M + \Delta M + O[(\delta/K)^2]$, where ΔM is the leading order correction to the stability matrix,

$$\Delta M = \delta\sin\theta_{d,0}\begin{pmatrix} \Delta\mathbb{M}_{(d+1)\times(d+1)} & 0_{(d+1)\times(N-d)} \\ 0_{(N-d)\times(d+1)} & 0_{(N-d)\times(N-d)} \end{pmatrix}, \tag{10}$$

with $\Delta\mathbb{M}$ defined as

$$\begin{pmatrix} -CT_{d,0}-T_{1,0} & T_{1,0} & 0 & \dots & CT_{d,0} \\ T_{1,0} & -T_{1,0}-T_{2,1} & T_{2,1} & 0 & \vdots \\ 0 & \ddots & \ddots & \ddots & 0 \\ \vdots & 0 & \ddots & \ddots & T_{d,d-1} \\ CT_{d,0} & \dots & 0 & T_{d,d-1} & -CT_{d,0}-T_{d,d-1} \end{pmatrix}, \tag{11}$$

where we introduced the notations $T_{i+1,i} \equiv \tan\theta_{i+1,i}$ and $CT_{d,0} \equiv \cot\theta_{d,0}$.

Let $\mathbf{u}^{(2)} \in \mathbb{R}^{N+1}$ be defined by $M\mathbf{u}^{(2)} = \lambda_2\mathbf{u}^{(2)}$. Then, the leading order correction to λ_2 is given by $\Delta\lambda_2 = \mathbf{u}^{(2)\top}\Delta M\mathbf{u}^{(2)}$. If the sign of $\Delta\lambda_2$ is negative (positive), then, to 1st order in δ, the stability of the power flow solution is enhanced (reduced). Below we discuss how $\mathrm{sgn}(\Delta\lambda_2)$ changes as a function of the position d of the additional connection. To achieve this, we distinguish the two cases $\tan\theta_{d,0} \geq 0$ and $\tan\theta_{d,0} \leq 0$.

When $\tan\theta_{d,0} \leq 0$, the matrix $\Delta\mathbb{M}$ is diagonal dominant [37] (since $\theta_{i+1,i} \in [-\pi/2, 0]$ we have $\tan\theta_{i+1,i} \leq 0$) with a strictly

positive diagonal. Hence ΔM (10) is either semi-positive or semi-negative definite depending exclusively on the sign of $\sin\theta_{d,0}$. In both cases the sign of $\Delta\lambda_2 = \mathbf{u}^{(2)^\top}\Delta M\mathbf{u}^{(2)}$ is well defined regardless of $\mathbf{u}^{(2)}$, and we have

$$\begin{cases} \Delta\lambda_2 \geq 0 & \text{for} \quad \theta_{d,0} \in [\pi/2, \pi] \Rightarrow \text{reduced stability}, \\ \Delta\lambda_2 \leq 0 & \text{for} \quad \theta_{d,0} \in [-\pi/2, 0] \Rightarrow \text{enhanced stability}. \end{cases} \tag{12}$$

When $\tan\theta_{d,0} \geq 0$, $\Delta\mathbb{M}$ is no longer diagonal dominant and it is not possible to determine the sign of $\Delta\lambda_2$ as directly as before. Instead we use $\mathbf{u}^{(2)} = (u_0^{(2)}, \ldots, u_N^{(2)})$ to compute $\mathbf{u}^{(2)^\top}\Delta M\mathbf{u}^{(2)}$ explicitly,

$$\begin{aligned} \Delta\lambda_2 = \; & -\delta\cos\theta_{d,0}\Big[\left(u_0^{(2)} - u_d^{(2)}\right)^2 \\ & + \tan\theta_{d,0}\sum_{i=0}^{d-1}\left(u_i^{(2)} - u_{i+1}^{(2)}\right)^2\tan\theta_{i+1,i}\Big]. \end{aligned} \tag{13}$$

The one dimensional nature of the model allows to express the difference $u_0^{(2)} - u_d^{(2)}$ as the telescopic sum $\sum_{i=0}^{d-1}(u_i^{(2)} - u_{i+1}^{(2)}) = u_0^{(2)} - u_d^{(2)}$. Using this identity we rewrite the term $(u_0^{(2)} - u_d^{(2)})^2$ entering Eq. (13) as

$$\begin{aligned} \left[\sum_{i=0}^{d-1}(u_i^{(2)} - u_{i+1}^{(2)})\right]^2 = \; & \sum_{i=0}^{d-1}\left(u_i^{(2)} - u_{i+1}^{(2)}\right)^2 \\ & +2\sum_{i=0}^{d-1}\sum_{j>i}(u_i^{(2)} - u_{i+1}^{(2)})(u_j^{(2)} - u_{j+1}^{(2)}). \end{aligned} \tag{14}$$

Substituting Eq. (14) in Eq. (13) finally yields

$$\begin{aligned} \Delta\lambda_2 = \; & -\delta\cos\theta_{d,0}\Big[2\sum_{i=0}^{d-1}\sum_{j>i}(u_i^{(2)} - u_{i+1}^{(2)})(u_j^{(2)} - u_{j+1}^{(2)}) \\ & + \tan\theta_{d,0}\sum_{i=0}^{d-1}(u_i^{(2)} - u_{i+1}^{(2)})^2\left(\tan\theta_{i+1,i} + \cot\theta_{d,0}\right)\Big]. \end{aligned} \tag{15}$$

Because M is a Jacobi matrix, it can be shown (See Appendix A) that the components of its eigenvector $\mathbf{u}^{(2)}$ are monotonously ordered. Thus $(u_i^{(2)} - u_{i+1}^{(2)})(u_j^{(2)} - u_{j+1}^{(2)}) \geq 0$ and the first term in Eq. (15) is positive. Furthermore, for $\tan\theta_{d,0} \geq 0$, it is possible to establish a sufficient condition on $\theta_{d,0}$ according to which the sign of $\Delta\lambda_2$ is known. Since all $\theta_{i+1,i}$ belong to $[-\pi/2, 0]$ and given the monotonicity of the tangent function over this interval, if $(\tan\theta^{\min} + \cot\theta_{d,0}) \geq 0$ where $\theta^{\min} = \min_{i\in\{0,\ldots,d-1\}}\theta_{i+1,i}$ then we also have $(\tan\theta_{i+1,i} + \cot\theta_{d,0}) \geq 0$ for $i \in \{0, 1, \ldots, d-1\}$. When this is the case we conclude that $\Delta\lambda_2 \propto -\cos\theta_{d,0}$. Thus, when $\tan\theta_{d,0} \geq 0$, the sign of $\Delta\lambda_2$ is directly given by $-\text{sgn}(\cos\theta_{d,0})$ if $\tan\theta_{d,0} \leq -\cot\theta^{\min}$. Inspecting Eq. (2) one sees that $\theta^{\min}$ is realized on the most loaded line prior to the network upgrade, that is on the line having the largest ratio of transmitted power over available capacity. Let $\langle q+1, q\rangle$ denote the line minimizing $\min_{i\in\{0,\ldots,d-1\}}\theta_{i+1,i}$ (i.e. the line where $P_i^\star/K_{i+1,i}$ is maximal), then the condition $\tan\theta_{d,0} \leq -\cot\theta^{\min}$ can be rewritten as

$$\tan\theta_{d,0} \leq \sqrt{K_{q+1,q}^2 - P_q^{\star 2}}/P_q^\star. \tag{16}$$

This defines a critical angle $\alpha \equiv \arctan\left[\sqrt{K_{q+1,q}^2 - P_q^{\star 2}}/P_q^\star\right] \in [0, \pi/2]$, such that

$$\begin{cases} \Delta\lambda_2 \leq 0 & \text{for} \quad \theta_{d,0} \in [0, \alpha] \Rightarrow \text{enhanced stability}, \\ \Delta\lambda_2 \geq 0 & \text{for} \quad \theta_{d,0} \in [-\pi, -\pi+\alpha] \Rightarrow \text{reduced stability}. \end{cases} \tag{17}$$

The size of the region $[\alpha, \pi/2] \bigcup [-\pi + \alpha, -\pi/2]$, where the evolution of the stability remains undetermined, vanishes as $P_q^\star/K_{q+1,q}$ when $P_q^\star/K_{q+1,q} \to 0$ since in this limit $\alpha \approx \pi/2 - P_q^\star/K_{q+1,q}$.

These results are summarized in Fig. 2. When the angle difference between the newly connected nodes satisfies $\theta_{d,0} \in [-\pi/2, 0]$, the additional line reduces the load on the most loaded line in the loop (i.e. line $\langle q+1, q\rangle$) and the stability of the power flow solution is enhanced. This is what one generally expects of line addition. Line addition can however worsen the operating conditions of the network and our theory highlights three different Braess scenarios how this may happen – by either increasing the load, by reducing $|\lambda_2|$, or both. The worst case scenario occurs when $\theta_{d,0} \in [\pi/2, \pi]$. Then, the additional line increases the power load on the most loaded line and the stability of the new solution is decreased. Paradoxical situations occur when $\theta_{d,0} \in [0, \alpha]$ (respectively $\theta_{d,0} \in [-\pi, -\pi+\alpha]$) as the load on the most loaded line increases (decreases) while the linear stability is enhanced (decreased). These three outcomes are three different manifestations of Braess's paradox in electric power transmission. We note that the chain model results also apply to the case of line addition in radial (tree like) networks as long as the new line connects two nodes on the same branch.

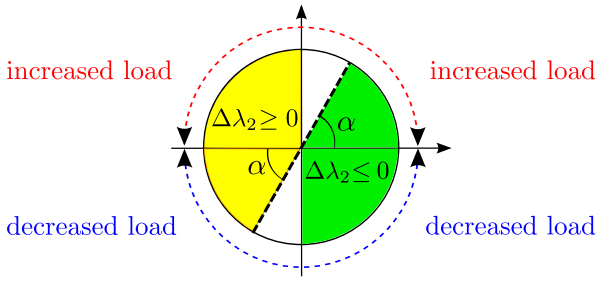

FIG. 2. (Color online) Impact of perturbative line addition on the linear stability of the power flow solution (green region, enhanced stability; yellow region, reduced stability) and on the load of the transmission lines (top quadrants, increased load; bottom quadrants, decreased loads) as a function of the value of $\theta_{d,0}$.

VI. EXTENSION TO COMPLEX NETWORKS.

To show how the mechanisms described above can lead to the loss of synchrony in more complex networks, we consider the electric power transmission grid discussed in Refs. [15, 16]. It has the same topology as the UK transmission network, and we take the same distribution of loads, generators and line capacities as in Ref. [15]. The general struc-

ture of the grid is that of a northern, importing zone connected to a southern, exporting zone via only two lines which are almost at full capacity [see Fig. 3 (left panel)]. It is obviously desirable to relieve these lines by adding another south-north transmission line.

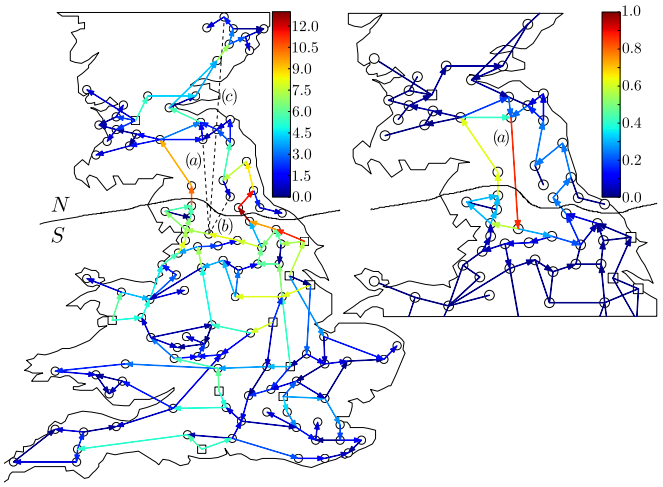

FIG. 3. (Color online) Left: UK transmission grid, 10 generators with power $P = 11$ (squares), 110 loads with $P = -1$ (circles) and uniform line capacity $K \equiv 13$. Power flows are represented by arrows and their magnitude is color coded. The dashed lines $(a) - (c)$ represent three different line additions considered and the solid line denotes the network partition into northern and southern zones. Right: Plot of the difference in power flows between the solutions after and before the addition of line (a) of capacity $\delta = 1.5$. Arrow heads are drawn only for power flow differences larger than 0.01.

The situation is in a way similar to our simple model, where the south plays the role of the generator and the north that of the loads. This is however only an analogy since the elongated UK grid is a meshed network and not a 1D model as considered above. In the case of a generic network, Eq. (15) becomes

$$\Delta\lambda_2 = \delta \sin\theta_{\alpha,\beta}\left[\sum_{\langle i,j\rangle} f_{ij}\left(u_i^{(2)} - u_j^{(2)}\right)^2 - \left(u_\alpha^{(2)} - u_\beta^{(2)}\right)^2 \cot\theta_{\alpha,\beta}\right], \tag{18}$$

with $f_{i,j} = K_{i,j}\sin\theta_{i,j}\sum_{l\geq 2}\left(u_i^{(l)} - u_j^{(l)}\right)\left(u_\alpha^{(l)} - u_\beta^{(l)}\right)\lambda_l^{-1}$ and where α and β are the nodes connected by the new line, $\langle i, j\rangle$ indicates the sum over all pairs of connected neighbors in the original network and $\mathbf{u}^{(l)}$ is the l^{th} eigenvector of the stability matrix (see Appendix B). After the upgrade, the power flowing through the line connecting nodes i and j becomes $P_{i,j} = K_{i,j}\sin\theta_{i,j} + \delta\sin\theta_{\alpha,\beta}\, f_{i,j}\cos\theta_{i,j}$. Following our work, a similar expression for the change in power flows resulting from the variation of the capacity of one line was used in Ref. [40] to investigate the effect of line failures.

In what follows we present examples of additions of new lines between the north and the south. Each illustrates the realization of one of the electric Braess paradoxes discussed above. We first add the dashed line (a) [Fig. 3], between two nodes having the angle difference $\theta_{\text{North}} - \theta_{\text{South}} \equiv \theta_{N,S} \approx 0.9\pi \in [\pi/2, \pi]$. For this choice, Fig. 2 predicts counter-intuitively, that power will flow from the north to the south through the new connection. This is numerically verified in Fig. 3 (right panel), which shows that adding the new line increases even further the load on the two original lines connecting the two zones - the power flow in the new line goes in the wrong direction. The effect is quantified in Fig. 4 a) as a function of the capacity of the new line. Both the loads on the original connection lines and the Lyapunov exponent λ_2 increase as a function of δ. Going beyond the validity of our perturbative approach, synchrony is lost in the interval $\delta \in [2.1, 5.2]$ (the gray region in Fig. 4 a), and is recovered at larger values of δ, where the stable operating state strongly differs from the unperturbed one. Synchrony is lost for $\delta \nearrow 2.1$ and $\delta \searrow 5.2$ as the power flow solutions become unstable ($\lambda_2 \to 0$), similarly to results reported in Ref. [26].

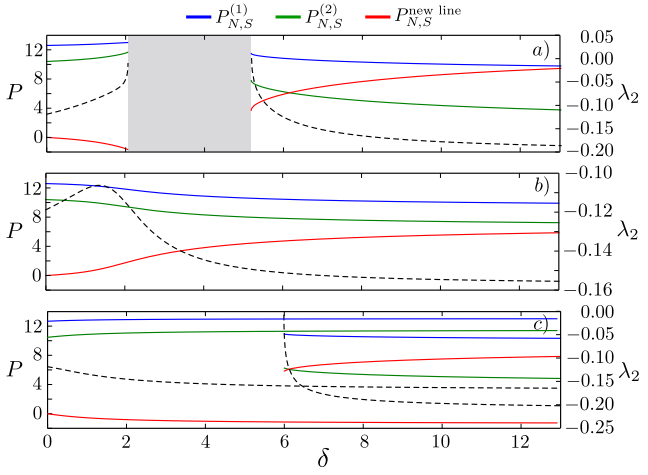

FIG. 4. (Color online) Lyapunov exponent (dashed) and power flowing through the lines connecting the north and south areas as a function of the capacity of the additional line δ. Each of the panels refers to one of the line additions represented in Fig. 3 (labels correspond to the labels of the additional lines in Fig. 3) and illustrates one of the three Braess scenarios identified in this work. Interestingly, panel c) shows the coexistence of two different stable solutions for $\delta \geq 5.98$.

The added line labeled by (b) [see Fig. 3] is chosen to connect two nodes such that $\theta_{N,S} \approx -0.9\pi \in [-\pi, -\pi/2]$. As can be seen in Fig. 4 b) power is flowing from the south to the north along this new line. Despite the associated reduction of the power flow on the two original lines, the Lyapunov exponent increases as predicted in Fig. 2. For larger added capacity, however, λ_2 reaches a maximum, then starts to decrease, and synchrony is never lost. This observation can be understood qualitatively in terms of our simple model: as the capacity of the new connection increases, the difference $\theta_{N,S}$, originally in the 3$^{\text{rd}}$ quadrant increases until eventually it reaches the 4$^{\text{th}}$ trigonometric quadrant for which the correction to λ_2 is expected to become negative.

We finally add line (c) [see Fig. 3] between two nodes with $\theta_{N,S} \approx 0.3\pi$. This time power flows through the new line from the north to the south. The loads on the original connections between the two zones, which were already close to saturation, increase further. Quite interestingly, the linear stability of the solution is improved, $\Delta\lambda_2 \leq 0$, despite this

load increase. The solution followed as δ is raised from 0 remains linearly stable in the whole capacity range investigated $\delta \in [0, 13]$. When the capacity of the additional line reaches 5.98 units of power, the numerical simulations also converge to another stable solution of the power flow equations [see Fig. 4 c)]. The behavior of λ_2 indicates that the new, large−δ solution becomes unstable ($\lambda_2 = 0$) when $\delta \searrow 5.98$. The regime $\delta \geq 5.98$ is an example of coexistence of multiple stable power flow solutions [31, 41–44].

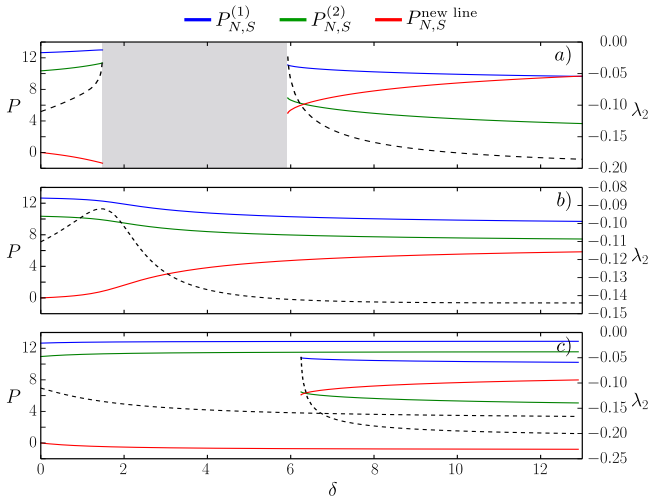

FIG. 5. (Color online) Lyapunov exponent (dashed) and power flowing though the lines connecting the north and south areas as a function of the capacity of the additional line δ, for the UK transmission grid in the case of line capacities uniformly distributed in the interval [9.75, 16.25]. Each panel refers to one of the line additions represented in Fig. 3 and illustrates one of the three Braess scenarios identified in this work.

To assess the robustness of the perturbation theory results we repeat the numerical simulations for the UK transmission grid including line capacity variations of ±25% with respect to the uniform case, $K \equiv 13$, presented above. We take line capacities uniformly distributed in the interval [9.75, 16.25] keeping the most loaded line crossing the north-south border at $K = 13$, and consider the same network upgrades discussed earlier. The numerical results presented in Fig. 5 are very similar to those of Fig. 4, indicating that the three different Braess scenarios identified for the uniform line capacity case are robust with respect to the significant capacity variations considered.

VII. CONCLUSION.

We classified the impact of a line addition in an AC power grid into four possible scenarios depending on the change in linear stability of the synchronous solution and on the change in power load on the lines. For the chain model, we showed that the effect of such network upgrades depends uniquely on the voltage angle difference between the nodes connected by the new line. This classification is summarized in Fig. 2, and we showed that it can be extended to meshed networks having the topology of transmission grids. In this case it is however less straightforward to predict from the unperturbed operational state which of the four scenarios will be realized.

We think that our theory has significantly deepened our understanding of the Braess paradox in electric power systems. More generally, it is based on rather generic models, which suggests that Braess paradoxes, in the form of weaker stability of the synchronous state after coupling addition, are ubiquitous in systems of coupled oscillators. Future works should attempt to extend this theory to the non pertubative regime of large line capacity and include dissipation effects which become important as voltage angle differences become large.

We thank R. Delabays for useful discussions. This work was supported by the Swiss National Science Foundation.

Appendix A: Jacobi matrices

1. Properties of Jacobi matrices.

In this section we list some of the properties of the eigenvalues and eigenvectors of Jacobi matrices. For further details and proofs of these results see Ref. [38]. Consider the following positive semi-definite, symmetric, tridiagonal matrix with strictly negative subdiagonals

$$J = \begin{pmatrix} a_1 & -b_1 & 0 & \dots & 0 \\ -b_1 & a_2 & -b_2 & 0 & \vdots \\ 0 & \ddots & \ddots & \ddots & 0 \\ \vdots & & \ddots & \ddots & -b_{n-1} \\ 0 & \dots & 0 & -b_{n-1} & a_n \end{pmatrix}, \qquad b_i > 0\,. \tag{A1}$$

Such matrices are also known as Jacobi matrices and have the property that their eigenvalues are distinct [38]. Furthermore, the principal minors of J (the k^{th} principal minor J is the truncated version of J consisting of $J_{i,j}$ with $i, j = 1, \dots, k \leq n$) satisfy the following recurrence relation

$$D_{k+1}(\lambda) = (a_{k+1} - \lambda)D_k(\lambda) - b_k^2 D_{k-1}(\lambda)\,, \tag{A2}$$

where $D_k(\lambda)$ is the characteristic polynomial of the k^{th} principal minor of J ($D_0(\lambda) = 1$ and $D_1(\lambda) = a_1 - \lambda$). In particular $D_n(\lambda)$ is the characteristic polynomial of J which vanishes when λ is equal to one of the eigenvalues $\lambda_1 < \lambda_2 < \dots < \lambda_n$ of J. It can be shown [38] that the sequence

$$\{D_{n-1}(\lambda), D_{n-2}(\lambda), \dots, D_1(\lambda), D_0(\lambda)\} \tag{A3}$$

contains $j - 1$ sign changes when evaluated at the j^{th} eigenvalue $\lambda = \lambda_j$.

If $\mathbf{u}^{(j)} = (u_1^{(j)}, \dots, u_n^{(j)})$ is the eigenvector of J associated to λ_j it is straightforward to show that the coefficients of $\mathbf{u}^{(j)}$ satisfy a recurrence relation which is similar to that of Eq. (A2)

$$\begin{aligned} & J\mathbf{u}^{(j)} = \lambda_j \mathbf{u}^{(j)}\,, \\ \Leftrightarrow\ & -b_{k-1}u_{k-1}^{(j)} + a_k u_k^{(j)} - b_k u_{k+1}^{(j)} = \lambda_j u_k^{(j)}\,, \\ \Leftrightarrow\ & b_k u_{k+1}^{(j)} = (a_k - \lambda_j)u_k^{(j)} - b_{k-1}u_{k-1}^{(j)}\,, \end{aligned} \tag{A4}$$

for $k \in \{1,\dots,n\}$ and $u_0^{(j)} = u_{n+1}^{(j)} = 0$. In fact one obtains that (A4) is fulfilled by

$$u_k^{(j)} \propto \frac{D_{k-1}(\lambda_j)}{b_1 \dots b_{k-1}}\,. \tag{A5}$$

Hence, given the sign property of the sequence $\{D(\lambda_j)\}$, it is clear that the components of the eigenvector $\mathbf{u}^{(j)}$ will have $j-1$ sign changes.

We mention a last property [38] of the eigenvectors of J which is useful for our electrical model. Given two eigenvectors $\mathbf{u}^{(j)}$ and $\mathbf{u}^{(i)}$ we have

$$\begin{aligned} -b_{k-1}u_{k-1}^{(j)} + a_k u_k^{(j)} - b_k u_{k+1}^{(j)} &= \lambda_j u_k^{(j)}\,, \\ -b_{k-1}u_{k-1}^{(i)} + a_k u_k^{(i)} - b_k u_{k+1}^{(i)} &= \lambda_i u_k^{(i)}\,. \end{aligned} \tag{A6}$$

Eliminating a_k one obtains

$$b_k(u_k^{(i)}u_{k+1}^{(j)} - u_{k+1}^{(i)}u_k^{(j)}) + b_{k-1}(u_k^{(i)}u_{k-1}^{(j)} - u_{k-1}^{(i)}u_k^{(j)}) = (\lambda_i - \lambda_j)u_k^{(j)}u_k^{(i)}\,, \tag{A7}$$

which summed over $k = 1, 2, \dots, l$ gives

$$b_l(u_l^{(i)}u_{l+1}^{(j)} - u_{l+1}^{(i)}u_l^{(j)}) = (\lambda_i - \lambda_j)\sum_{k=1}^{l} u_k^{(j)}u_k^{(i)}\,. \tag{A8}$$

2. Connection to the chain model.

The matrix $-M$ constructed for our chain model prior to the line addition is a Jacobi matrix with the additional property that since $a_i = b_i + b_{i-1}$ its first eigenvalue λ_1 is equal to zero and the corresponding eigenvector is $\mathbf{u}^{(1)} = (1,\dots,1)$. Thus, applying Eq. (A8) to $-M$ with $j = 1$ and $i = 2$ yields a relation between any two consecutive components of $\mathbf{u}^{(2)}$

$$(u_l^{(2)} - u_{l+1}^{(2)}) = \frac{\lambda_2}{b_l}\sum_{k=1}^{l} u_k^{(2)}\,. \tag{A9}$$

Additionally, according to the properties of Jacobi matrices, there will be only one sign change in the list of the coefficients of $\mathbf{u}^{(2)}$ which therefore will have the form $(\pm,\dots,\pm,\mp,\dots,\mp)$. Lastly, the orthogonality relation between $\mathbf{u}^{(1)}$ and $\mathbf{u}^{(2)}$ implies that

$$\mathbf{u}^{(1)\top}\mathbf{u}^{(2)} = 0 \quad \Leftrightarrow \quad \sum_{k=1}^{n} u_k^{(2)} = 0\,. \tag{A10}$$

Using Eq. (A10) and the sign properties of the coefficients of $\mathbf{u}^{(2)}$ suffices to see that Eq. (A9) leads to the conclusion that the components of $\mathbf{u}^{(2)}$ are monotonously ordered (i.e. for any $i > j$ we either have $u_i^{(2)} \geq u_j^{(2)}$ or $u_i^{(2)} \leq u_j^{(2)}$).

Appendix B: Perturbation theory for a generic graph

In this section we extend the calculation of the leading order correction to the Lyapunov exponent λ_2 resulting from the addition of a new line to the case of a generic electric network.

Given a generic network of N nodes and lines of capacity $K_{i,j}$, let $\{\theta_i\}$ and $\{\tilde{\theta}_i\}$ respectively denote the solutions of the power flow equations (1) before and after the addition of a line of capacity $\delta \ll K_{i,j}$ between nodes α and β. Assuming the $\tilde{\theta}_i$'s are small deviations of the unperturbed solution ($\tilde{\theta}_i \approx \theta_i + \delta\theta_i$ with $|\delta\theta_i| \ll 1$), we expand the power flow equations to leading order in δ

$$\begin{aligned} 0 &= \sum_{l\sim i} K_{l,i}\cos(\theta_l - \theta_i)(\delta\theta_l - \delta\theta_i) \quad i \neq \alpha,\beta\,, \\ 0 &= \sum_{l\sim\alpha,\, l\neq\beta} K_{l,\alpha}\cos(\theta_l - \theta_\alpha)(\delta\theta_l - \delta\theta_\alpha) + \delta\sin(\theta_\beta - \theta_\alpha) \quad i = \alpha\,, \\ 0 &= \sum_{l\sim\beta,\, l\neq\alpha} K_{l,\beta}\cos(\theta_l - \theta_\beta)(\delta\theta_l - \delta\theta_\beta) + \delta\sin(\theta_\alpha - \theta_\beta) \quad i = \beta\,. \end{aligned} \tag{B1}$$

Eqs. (B1) can be rewritten using the stability matrix, M [defined below Eq. (5)], of the system prior to the line addition

$$M\boldsymbol{\delta\theta} = \delta\sin\theta_{\alpha,\beta}\boldsymbol{\nu}\,, \tag{B2}$$

where $\boldsymbol{\delta\theta} = (\delta\theta_1,\dots,\delta\theta_N)$ and $\boldsymbol{\nu}$ is the N dimensional vector whose i^{th} component is equal to $\nu_i = \delta_{i,\alpha} - \delta_{i,\beta}$.

M, being a real symmetric matrix, is diagonalized by an orthogonal matrix T whose l^{th} column is the l^{th} eigenvector, $\mathbf{u}^{(l)}$, of M. Furthermore, the $U(1)$ symmetry of the power flow equations implies that one of the eigenvalues of M is null ($\lambda_1 = 0$ assocuated to $\mathbf{u}^{(1)} = (1,\dots,1)/\sqrt{N}$). Since M is singular it cannot be inverted. However, Eq. (B2) can be solved for the $\delta\theta_i$'s by using the Moore-Penrose pseudoinverse of M defined as

$$M^{-1} = T\begin{pmatrix} 0 & & & \\ & \lambda_2^{-1} & & \\ & & \ddots & \\ & & & \lambda_N^{-1} \end{pmatrix}T^\top\,, \tag{B3}$$

where $T = (\mathbf{u}^{(1)},\dots,\mathbf{u}^{(N)})$ and the λ_l's are the eigenvalues of M. M^{-1} is such that $M^{-1}M = M^{-1}M = \mathbb{1} - \mathbf{u}^{(1)}\mathbf{u}^{(1)\top}$, where $\mathbf{u}^{(1)}\mathbf{u}^{(1)\top}$ is equal to the $N\times N$ matrix having $1/N$ for all it's entries. Multiplying (B2) by M^{-1} yields

$$\begin{pmatrix} \delta\theta_1 \\ \vdots \\ \delta\theta_N \end{pmatrix} - \frac{1}{N}\begin{pmatrix} \sum_l \delta\theta_l \\ \vdots \\ \sum_l \delta\theta_l \end{pmatrix} = \delta\sin\theta_{\alpha,\beta}\begin{pmatrix} M_{1,\alpha}^{-1} - M_{1,\beta}^{-1} \\ \vdots \\ M_{N,\alpha}^{-1} - M_{N,\beta}^{-1} \end{pmatrix}. \tag{B4}$$

The difference of $\delta\theta_i$'s between any two nodes is given by

$$\delta\theta_i - \delta\theta_j \equiv \epsilon_{i,j} = \delta\sin\theta_{\alpha,\beta}\left[\left(M_{i,\alpha}^{-1} - M_{i,\beta}^{-1}\right) - \left(M_{j,\alpha}^{-1} - M_{j,\beta}^{-1}\right)\right], \tag{B5}$$

where the term $\sum_l \delta\theta_l$ drops due to the global rotational invariance of the power flow solution. Finally, Eq. (B5) can be expressed in terms of the eigenvectors of M making use of (B3). This yields

$$\epsilon_{i,j} = \delta\sin\theta_{\alpha,\beta}\sum_{l\geq 2}\left(u_i^{(l)} - u_j^{(l)}\right)\left(u_\alpha^{(l)} - u_\beta^{(l)}\right)\lambda_l^{-1}\,, \tag{B6}$$

for any node i connected to node j. Having established the correction to the power flow solution (B6), it is straight forward to compute the leading correction to the stability matrix,

ΔM, and to obtain the correction of the Lyapunov exponent $\Delta\lambda_2 = \mathbf{u}^{(2)\top}\Delta M\mathbf{u}^{(2)}$. The final expression for $\Delta\lambda_2$ in the case of a generic network is presented in Eq. (18).

[1] Y. Kuramoto, in *International Symposium on Mathematical Problems in Theoretical Physics*, Vol. 39, pp. 420-422 (Springer, New York, 1975).
[2] S. H. Strogatz, Nature **410**, 268 (2001).
[3] J. A. Acebrón, L. L. Bonilla, C. J. Pérez Vicente, F. Ritort, and R. Spigler, Rev. Mod. Phys. **77**, 137 (2005).
[4] K. Wiesenfeld, P. Colet, and S. H. Strogatz, Phys. Rev. Lett. **76**, 404 (1996).
[5] A. T. Winfree, Journal of Theoretical Biology **16**, 15 (1967).
[6] B. Ermentrout, Journal of Mathematical Biology **29**, 571 (1991).
[7] S. H. Strogatz, D. M. Abrams, A. McRobie, B. Eckhardt, and E. Ott, Nature **438**, 43 (2005).
[8] M. A. Arbib, ed., *The Handbook of Brain Theory and Neural Networks*, 2nd ed. (MIT Press, Cambridge, MA, USA, 2002).
[9] Y. Kuramoto, *Chemical Oscillations, Waves, and Turbulence* (Springer Berlin Heidelberg, 1984).
[10] F. Dörfler and F. Bullo, in *IEEE 51st Annual Conference on Decision and Control* (2012) pp. 7157–7170.
[11] F. Dörfler, M. Chertkov, and F. Bullo, Proceedings of the National Academy of Sciences **110**, 2005 (2013).
[12] A. E. Motter, S. A. Myers, M. Anghel, and T. Nishikawa, Nat Phys **9**, 191 (2013).
[13] S. Backhaus and M. Chertkov, Physics Today **66**, 42 (2013).
[14] T. Nishikawa and A. E. Motter, Phys. Rev. E **73**, 065106 (2006).
[15] D. Witthaut and M. Timme, New Journal of Physics **14**, 083036 (2012).
[16] D. Witthaut and M. Timme, Eur. Phys. J. B **86**, 377 (2013).
[17] D. Braess, Unternehmensforschung **12**, 258 (1968).
[18] D. Braess, A. Nagurney, and T. Wakolbinger, Transportation Science **39**, 446 (2005).
[19] J. E. Cohen and P. Horowitz, Nature **352**, 699 (1991).
[20] S. Blumsack, L. B. Lave, and M. Ilić, The Energy Journal **28**, 73 (2007).
[21] P. Kundur, N. J. Balu, and M. G. Lauby, *Power system stability and control*, Vol. 7 (McGraw-hill New York, 1994).
[22] A. J. Wood, B. F. Wollenberg, and G. B. Sheblé, *Power generation, operation, and control* (John Wiley & Sons, New York, 2013).
[23] L. M. Pecora and T. L. Carroll, Phys. Rev. Lett. **80**, 2109 (1998).
[24] K. S. Fink, G. Johnson, T. Carroll, D. Mar, and L. Pecora, Phys. Rev. E **61**, 5080 (2000).
[25] E. Mallada and A. Tang, in *50th IEEE Conference on Decision and Control* (2011) pp. 7729–7734.
[26] D. Manik, D. Witthaut, B. Schäfer, M. Matthiae, A. Sorge, M. Rohden, E. Katifori, and M. Timme, Eur. Phys. J. Special Topics **223**, 2527 (2014).
[27] P. J. Menck, J. Heitzig, J. Kurths, and H. J. Schellnhuber, Nat. Commun. **5**, 3969 (2014).
[28] A. Arenas, A. Daz-Guilera, J. Kurths, Y. Moreno, and C. Zhou, Physics Reports **469**, 93 (2008).
[29] G. Filatrella, A. H. Nielsen, and N. F. Pedersen, The European Physical Journal B **61**, 485 (2008).
[30] N. Chopra and M. Spong, IEEE Transactions on Automatic Control **54**, 353 (2009).
[31] R. Delabays, T. Coletta, and P. Jacquod, Journal of Mathematical Physics **57**, 032701 (2016), 10.1063/1.4943296.
[32] In our convention $P_{i,j} = K_{i,j}\sin(\theta_i - \theta_j)$, $P_{i,j} > 0$ (respectively $P_{i,j} < 0$) means that a power of $|P_{i,j}|$ is flowing from node i to node j (respectively from node j to node i).
[33] S. H. Strogatz, Physica D: Nonlinear Phenomena **143**, 1 (2000).
[34] A. Jadbabaie, N. Motee, and M. Barahona, in *Proceedings of the American Control Conference*, Vol. 5 (2004) pp. 4296–4301.
[35] R. E. Mirollo and S. H. Strogatz, Physica D: Nonlinear Phenomena **205**, 249 (2005).
[36] F. Dörfler and F. Bullo, SIAM Journal on Control and Optimization **50**, 1616 (2012).
[37] R. A. Horn and C. R. Johnson, *Matrix Analysis* (Cambridge University Press, New York, NY, USA, 1986).
[38] G. M. L. Gladwell, ed., *Inverse Problems in Vibration* (Springer, Berlin, 2005).
[39] Gershgorin circle theorem ensures that every eigenvalue of a matrix M is contained in at least one of the discs centered at $M_{i,i}$ and of radius $\sum_{j\neq i}|M_{i,j}|$ (see Ref. [37]).
[40] D. Witthaut, M. Rohden, X. Zhang, S. Hallerberg, and M. Timme, arXiv preprint arXiv:1510.08976 (2015).
[41] A. Korsak, Power Apparatus and Systems, IEEE Transactions on **PAS-91**, 1093 (1972).
[42] N. Janssens and A. Kamagate, International Journal of Electrical Power & Energy Systems **25**, 591 (2003).
[43] J. Ochab and P. F. Góra, Acta Physica Polonica B, Proceedings Supplement, **3(2)**, 453 (2010).
[44] D. Mehta, N. S. Daleo, F. Dörfler, and J. D. Hauenstein, Chaos **25**, 053103 (2015).